Metastable GPCR dimers trigger the basal signal by recruiting G-proteins

Rinshi S. Kasai[1], Takahiro K. Fujiwara[2], and Akihiro Kusumi[3]*

[1]Institute for Frontier Life and Medical Sciences and [2]Institute for Advanced Study, Institute for Integrated Cell-Material Sciences (KUIAS-iCeMS), Kyoto University, Kyoto 606-8507, Japan. [3]Membrane Cooperativity Unit, Okinawa Institute of Science and Technology Graduate University (OIST), Onna-son, Okinawa, 904-0495 Japan.

*To whom all correspondence should be addressed:
Akihiro Kusumi
e-mail: akihiro.kusumi@oist.jp
Ph: 011-81-98-966-1373, Fx: 011-81-98-966-1062

G-protein-coupled receptors (GPCRs) constitute the largest family of integral membrane proteins in the human genome and are responsible for various important signaling pathways for vision, olfaction, gustation, emotion, cell migration, etc. A distinct feature of the GPCR-family proteins is that many GPCRs, including the prototypical GPCR, β2-adrenergic receptor (β2AR), elicit low levels of basal constitutive signals without agonist stimulation, which function in normal development and various diseases[1-3]. However, how the basal signals are induced is hardly known. Another general distinctive feature of GPCRs is to form metastable homo-dimers, with lifetimes on the order of 0.1 s, even in the resting state. Here, our single-molecule-based quantification[4] determined the dissociation constant of β2AR homo-dimers in the PM (1.6 ± 0.29 copies/μm^2) and their lifetimes (83.2 ± 6.4 ms), and furthermore found that, in the resting state, trimeric G-proteins were recruited to both β2AR monomers and homo-dimers. Importantly, inverse agonists, which suppress the GPCR's basal constitutive activity, specifically blocked the G-protein recruitment to GPCR homo-dimers, without affecting that to monomers. These results indicate that the G-proteins recruited to transient GPCR homo-dimers are responsible for inducing their basic constitutive signals. These results suggest novel drug development strategies to enhance or suppress GPCR homo-dimer formation.

β2AR forms metastable homo-dimers

Single-molecule imaging-tracking revealed that β2AR (tagged with ACP at the N-terminus and labelled with ATTO594; **Extended Data Fig. 1**) undergoes thermal diffusion, and often forms transient homo-dimers, undergoing rapid interconversions between monomers and dimers continually, as found for other GPCRs (**Fig. 1a, Extended Data Fig. 2a**)[4-8]. Every time we found a β2AR dimer, we measured the dimer duration, and after observing many dimers, we obtained the distribution of dimer durations (**Fig. 1b, Extended Data Fig. 2d**). The histogram could be fitted by a single exponential function, providing the exponential dimer lifetime of 99 ms (throughout this report, all statistical parameters, including SEM, and the number of experiments are summarised in

50 **Extended Data Tables 1-4**; all observations were performed at 37°C). The lifetime value obtained
51 in this manner, termed $\tau_{observed}$, was corrected for the photobleaching lifetime and incidental
52 colocalisation lifetime (this method was used for evaluating all of the lifetimes investigated in the
53 present research; see **Methods**), giving a dimer lifetime τ of 83.2 ± 6.4 ms (**Fig. 1c**). The dimer
54 lifetime obtained at a time resolution of 4 ms (250 Hz) was 78.8 ± 10.7 ms, after corrections for
55 photobleaching and incidental colocalisation lifetime (**Extended Data Fig. 3, Fig. 1c**), which is
56 statistically indistinguishable from the dimer lifetime of 83.2 ms evaluated from 30-Hz observations.
57 This result indicates that a frame rate of 30 Hz is sufficiently fast for evaluating the homo-dimer
58 lifetime of β2AR. Together, these results demonstrate that the β2AR homo-dimers are indeed quite
59 metastable, turning into monomers in a matter of 80 ms, and then quite readily forming another
60 dimer with a different partner molecule (**Extended Data Fig. 2a**).
61
62 **2D-dissociation constant for β2AR dimers**
63 Using our single-molecule-based "super-quantification" method[4], we obtained the 2-dimensional
64 dissociation constant (2D-K_D) of β2AR homo-dimers in the PM of living cells, which was 1.6 ± 0.29
65 copies/μm^2 (**Fig. 2a, Extended Data Fig. 2b**; see **Methods**). This value is comparable to the
66 2D-K_D of another GPCR, formyl-peptide receptor (FPR), which was 3.6 copies/μm^2 (in fact, this was
67 the first determination of the 2D-K_D in the PM of living cells)[4].
68 Under physiological conditions, β2AR is expressed at number densities of 16 ~ 260 copies/μm^2,
69 depending on the cell type[9,10]. From the 2D-K_D determined here, we conclude that 12 ~ 240
70 copies/μm^2 exist as dimers and 4 ~ 20 copies/μm^2 exist as monomers at any moment; *i.e.*, 75 ~
71 92% of β2AR molecules exist as homo-dimers at any moment, although dimers and monomers are
72 interconverting rapidly (with a dimer lifetime of ~80 ms). In contrast, FPR is mainly expressed in
73 neutrophils, and an average of about 6,000 copies of FPR copies exist in the PM of a single
74 neutrophil[11]. Assuming that the neutrophil surface area is 1,300 μm^2 (approximated by a sphere with
75 a radius of 10 μm, providing a number density of ~4.6 FPR copies/ μm^2) and based on the 2D-K_D,
76 3,200 copies of FPR would exist as monomers and 2,800 copies as dimers; namely, 54% of FPR
77 molecules are dimers, which is about two-thirds of the dimer fraction of β2AR. Note that, even under

78 the conditions where the dimer population dominates (*i.e.*, at higher expression levels), the dimer
79 lifetimes do not change and remain on the order of 0.1 s. Only the monomer lifetimes are shortened
80 at higher expression levels.
81
82 **Direct detection of β2AR dimers by the BiFC method**
83 Thus far, we have detected dimers by the colocalisation of two single molecules, which reveals the
84 close encounters of molecules in the space scale of 220 nm, a distance much greater than the
85 molecular scale. Therefore, in this method, the incidental approaches of two molecules were
86 evaluated and subtracted. To ascertain the molecular-level interactions (dimers), we employed
87 YFP-based bimolecular fluorescence complementation (BiFC; meanwhile, our attempt to detect
88 FRET did not work, perhaps because the distance between the probes attached to two C-termini was
89 too far for FRET)[4,12]. In BiFC, two potentially interacting proteins are fused to the N- and C-terminal
90 half-molecules of YFP. If the proteins of interest form dimers, then YFP may be reconstituted and
91 emit fluorescence signals (see **Methods**). Thus, if BiFC occurs, it would lend strong support for the
92 formation of β2AR dimers.
93 To quantitatively examine BiFC, we varied the expression levels of β2AR. With an increase in
94 the number density of expressed molecules (determined by the signal from ATTO594 bound to ACP;
95 the ATTO594/ACP ratio is >0.95[13]), the number density of the BiFC spots of β2AR increased,
96 whereas the BiFC-spot number density of the monomer reference molecule, ACP-TM, increased only
97 slightly (**Fig. 2b; Extended Data Fig. 2c**). This result indicates that β2AR forms directly-bound
98 dimers.
99
100 **Inverse agonists reduce the β2AR dimer affinity**
101 Treatments with the inverse agonists ICI-118,551 (ICI) and Timolol reduced the β2AR dimer lifetime
102 (0.74x and 0.69x, respectively; **Fig. 1c, Extended Data Fig. 2d**), whereas ICI increased the 2D-K_D
103 of β2AR by a factor of 2.1 (lowered the β2AR dimer affinity; **Fig. 1c**), indicating that inverse agonists
104 reduce the β2AR dimer affinity. Meanwhile, the addition of the agonist isoproterenol (Iso) prolonged
105 the dimer lifetime significantly (1.55x) (**Fig. 1c; Extended Data Fig. 2d**). Cholesterol reportedly

106 modulates GPCR functions[14], but in our experiments, mild cholesterol depletion by
107 methyl-β-cyclodextrin (MβCD) treatment did not affect the dimer lifetime (**Fig. 1c**).
108 Since the inverse agonists suppressed the basal constitutive GPCR signaling, and we found
109 that they also reduced the β2AR dimer lifetime, we next examined the dimer lifetimes of the β2AR
110 mutants with high and low basal activities in the resting state (HBA and LBA mutants, representing
111 E268A and C327R mutants, respectively[15,16]). The HBA mutant exhibited a 1.78x longer dimer
112 lifetime, and interestingly, after the inverse-agonist addition, it was reduced to the dimer lifetime of
113 the wild-type receptor (**Fig. 1c; Extended Data Fig. 2d**). Meanwhile, the LBA mutant exhibited a
114 0.74x shorter dimer lifetime than that of the wild-type receptor, and the agonist addition did not
115 affect it (**Fig. 1c; Extended Data Fig. 2d**).
116 Strikingly, the dimer lifetimes of WT-β2AR after the addition of inverse agonists were quite
117 comparable to those of the LBA mutant, and the dimer lifetime of WT-β2AR after the addition of the
118 agonist isoproterenol was comparable to that of the HBA mutant. These results suggest that the
119 β2AR conformations would be quite different after the binding of the inverse agonists and the
120 agonist isoproterenol, as compared with those before their additions, possibly resembling the
121 conformations of the LBA and HBA mutants, respectively, and detectable as changes in the
122 homo-dimer lifetimes.
123
124 **The basal constitutive activity of β2AR**
125 We confirmed the basal constitutive activity of β2AR, as well as the effects of the β2AR agonist
126 isoproterenol and the inverse agonists ICI-118,551 and Timolol, by measuring the changes in the
127 cytoplasmic cAMP levels in the L-cell line stably expressing β2AR at higher levels (**Extended Data**
128 **Fig. 4, Extended Data Table 4**). The addition of the agonist isoproterenol to the cells increased
129 the cAMP level by a factor of ~4, relative to the control. Meanwhile, the addition of the inverse
130 agonists ICI-118,551 and Timolol reduced the cAMP levels by factors of 1.9 and 1.3 (53 and 76% of
131 the control), respectively, showing the presence of the basal constitutive activity of β2AR and the
132 effectiveness of the inverse agonists, ICI-118,551 and Timolol, for strongly reducing this basal
133 activity.

134

135 **Trimeric G proteins are recruited to both β2AR monomers and dimers**

136 The presence of the basal constitutive activity of β2AR suggests that a stimulatory trimeric G-protein
137 might be recruited to β2AR in the resting state. Therefore, we examined whether Gαs and Gβ
138 (conjugated with mGFP) are recruited to β2AR monomers or dimers, by examining their
139 colocalisations. Using L cells expressing both β2AR (ATTO594-ACP-β2AR) and Gαs or Gβ, we found
140 that, even in resting cells, Gαs and Gβ were recruited to both β2AR monomers and dimers (**Fig. 3a;**
141 **Supplementary Videos 1 and 2**).

142 The recruitment frequencies of Gαs and Gβ to β2AR monomers and dimers were measured
143 (per sec per μm^2) and then normalised by the number densities of Gαs (or Gβγ) and β2AR protomers
144 in the PM (normalised frequencies; **Fig. 3b, c; Extended Data Table 3**)[17]. In resting cells, both
145 Gαs and Gβ molecules were recruited to β2AR monomers or dimers equally well, suggesting that
146 (non-stimulated) β2AR monomers and/or dimers might induce intracellular Gs-dependent signals
147 even in the resting state, which would lead to the basal constitutive activity of β2AR.

148 The exponential dwell lifetimes of G proteins on β2AR were on the order of 50 ~ 60 ms for all
149 of the combinations of Gαs and Gβ molecules vs β2AR monomers and dimers (**Extended Data Fig.**
150 **5**). However, these durations are only the maximal estimates of the dwell lifetimes of Gαs and Gβ
151 molecules on β2AR monomers and dimers, due to the present instrumental limitations of detecting
152 short binding durations.

153 Notably, the treatment of the cells with the agonist, isoproterenol, did not change the
154 recruitment frequencies in any combinations of Gαs and Gβ vs β2AR monomers and dimers,
155 although it significantly enhanced the cytoplasmic cAMP level (**Extended Data Fig. 4, Extended**
156 **Data Table 4**). This result is quite surprising, but it suggests that the isoproterenol-induced β2AR
157 conformation enhanced its GEF activity, rather than increasing the on-rate of G protein binding to
158 β2AR.

159

160 **Inverse agonists specifically block G-protein recruitment to β2AR dimers**

161 Next, we examined the effects of the inverse agonists. The recruitment of Gαs and Gβ to β2AR

162 dimers was almost completely blocked, whereas that to β2AR monomers was unaffected (**Fig. 3b,**
163 **c**). This result unequivocally shows that β2AR dimers are responsible for the basal constitutive
164 activity of β2AR. Furthermore, it demonstrates that the inverse agonists work by blocking the
165 recruitment of stimulatory G-proteins to β2AR dimers, perhaps by inducing β2AR conformational
166 changes in the binding sites for G-proteins, rather than blocking the β2AR dimerisation (although, as
167 already described, the dimer affinity of the inverse agonist-bound β2AR is lower, resembling the LBA
168 mutant, and thus inverse agonists might change the GPCR conformations in two ways: lowering the
169 GPCR dimer affinity and modulating the G-protein binding sites).

170 To further confirm that β2AR dimers trigger downstream signaling without an agonist, and to
171 detect the basal dimer signal at the β2AR expression levels used for single-molecule experiments,
172 we examined whether artificially-induced stable β2AR dimers could elicit the downstream signal. To
173 detect the downstream signal at very low expression levels of β2AR, which are necessary for
174 detecting dimers by single-molecule imaging, and also to detect the signal in a different manner,
175 rather than observing the cAMP level again (**Extended Data Fig. 4**), we examined the intracellular
176 Ca^{2+} mobilisation, which could occur further downstream from the cAMP amplification[18]. The
177 induction of the artificially-induced stable β2AR (conjugated to FKBP) dimers by the FKBP-A20187
178 dimerisation system indeed elicited Ca^{2+} mobilisation (**Extended Data Fig. 6**). This result further
179 confirmed that β2AR dimers could trigger the downstream signals without agonist stimulation.
180

181 **Discussion**

182 All of the class-A GPCRs examined thus far, including β2AR examined here and by others[5], FPR, D2
183 dopamine receptor, M1 muscarinic receptor, and α1AR, form metastable dimers with lifetimes on the
184 order of 0.1 s in the non-stimulated state[4-8]. Therefore, we propose that the dynamic equilibrium
185 between monomers and homo-dimers is a common characteristic property of the class-A GPCRs.
186 The homo-dimerisation of GPCRs without any noticeable amino-acid homologies suggests that,
187 through evolution, GPCRs changed almost all of their amino acids, but conserved the physical ability
188 to form transient homo-dimers. This infers that these dynamic dimers are critical for some of the
189 GPCR functions.

190 GPCRs are distinct among other receptors, in that under non-stimulated conditions GPCRs
191 maintain the low basal constitutive activity, which can be inhibited by inverse agonists. The basal
192 activities of GPCRs are implied in normal development and various diseases[1-3]. Therefore, we
193 examined the possibility that the function of the GPCR dimers is to induce the basal constitutive
194 activity in resting cells (without agonists), and obtained three unexpected, surprising findings. First,
195 both β2AR monomers and dimers continually recruit G proteins, one molecule after another, even in
196 the resting state. Second, the G-protein recruitment frequencies in the resting state are about the
197 same in the presence of the agonist. Third, more importantly, the inverse agonists specifically and
198 almost completely blocked the recruitment of Gαs and Gβ to β2AR dimers, without affecting their
199 recruitment frequencies to β2AR monomers (**Fig. 3b, c**). The third result unequivocally shows that
200 the G proteins bound to β2AR dimers, and not monomers, in the resting state are responsible for
201 triggering the β2AR's basal constitutive activity, which is sensitive to inverse agonism. It further
202 suggests that the binding of the inverse agonists to β2AR induces conformational changes that
203 decrease the β2AR dimer affinities for G proteins (**Fig. 2a**) and at the same time, hide the binding
204 site(s) for G proteins in the dimer conformations.
205 Although the function of the GPCR dimers is to maintain the basal constitutive activity, it is
206 critically important to realise that the GPCR dimers are metastable with lifetimes on the order of 0.1
207 s. Therefore, the GPCR dimers are dispersing continually, forming new dimers with other partner
208 molecules all the time. In cells, this allows the basal constitutive activities of GPCRs to be maintained
209 at certain levels, and yet the levels of the basal GPCR signals (the average number density of GPCR
210 dimers at any time) are regulated globally, by modulating the GPCR number density by varying the
211 expression levels of the GPCR, and locally, by temporarily and spatially varying the actin-based
212 membrane skeleton and the membrane curvature[5,19-21]. In addition, the metastable GPCR dimers
213 might play important roles in the activation of G proteins after the agonist addition.
214 The present results suggest that the major functions of some of the orphan GPCRs might be
215 performed by the basal activities induced by their homo-dimers, as the GPCR family includes many
216 orphan receptors[3,22]. Based on the results described in this report, we strongly suggest the pursuit of
217 drug development strategies that emphasise the generation of more inverse agonists for various

GPCRs, as well as drugs that enhance or suppress GPCR homo-dimer formation.

Online content

Any methods, additional references, Nature Research reporting summaries, source data, extended data, supplementary information, acknowledgements, peer review information; details of author contributions and competing interests; and statements of data and code availability are available.

Acknowledgements

We thank Prof. Hajime Fujisawa of Nagoya University for providing mouse L cells, Prof. Tatsuya Haga of Gakushuin University for providing the cDNAs encoding β2AR and Gα, Prof. Tobias Meyer of Stanford University for providing the cDNA encoding YFP-FKBP through Addgene (plasmid 201751), Prof. Michiyuki Matsuda of Kyoto University for the excellent suggestion about the method for establishing cell lines stably expressing target proteins at high levels, Assoc. Prof. Akira Hattori for the use of the PerkinElmer time-resolved fluorescence resonance energy transfer reader, EnVision Xcite, for the cAMP measurement, Drs. Taka-Aki Tsunoyama of OIST, Ko Hirosawa of Gifu University, Prof. Kenichi Suzuki of Gifu University, and all of the members of the Kusumi laboratory for valuable discussions, suggestions, and support, and Mr. Koji Kanemasa of incomings for assistance with figure preparation. This work was supported by Grants-in-Aid for Scientific Research from the Japan Society for the Promotion of Science (Kiban C to R.S.K. [17K07333], Wakate B to R.S.K. [26870292], Kiban S to R.S.K. [Co-PI, 18H05269], and Kiban B to R.S.K. [Co-PI, 17H03666], Kiban B to T.K.F. [16H04775], and Kiban S to A.K. [16H06386]), Grants-in-Aid for Innovative Areas (Molecular Engine) from the Ministry of Education, Culture, Sports, Science, and Technology (MEXT) of Japan to R.S.K. [18H05424], and the Joint Research Program of Biosignal Research Center of Kobe University to R.S.K. [301002]. WPI-iCeMS of Kyoto University is supported by the World Premier Research Center Initiative (WPI) of the MEXT.

Author contributions

R.S.K. performed the single fluorescent-molecule tracking experiments and biochemical experiments. R.S.K., T.K.F., and A.K. developed and built the single-molecule imaging station. T.K.F. developed the analysis software. R.S.K. and A.K. conceived and formulated the project, evaluated and discussed the data, and wrote the manuscript, and all authors participated in revising the manuscript.

254 # Methods

255 **Cell culture, cDNA construction and expression in L cells, and treatment of cells**
256 **with agonists and inverse agonists.**

257 L cells (a kind gift from H. Fujisawa of Nagoya University), which do not express β2AR [23],
258 were confirmed to be free of mycoplasma contamination using MycoAlert (Lonza), and were
259 routinely cultured in Dulbecco's Minimum Essential Medium (DMEM; Sigma-Aldrich)
260 supplemented with 10% (v/v) FBS (Sigma-Aldrich), 100 units/ml penicillin (Wako), and 0.1
261 mg/ml streptomycin (Wako). Human β2AR was fused at its N-terminus to the ACP- or
262 Halo7-tag protein (NEB and Promega, respectively) at the cDNA level, and cloned into the
263 expression plasmid pEGFP-N1 (Clontech) after the removal of the cDNA region encoding
264 EGFP. The ACP- and Halo7-tag proteins do not induce dimerisation[12,24]. For the genetic
265 conjugation of mGFP to Gαs, the mGFP cDNA was inserted between the region encoding the
266 71st and 82nd amino acids of mouse Gαs (Origene) in the pcDNA3.1 (+) vector
267 (Invitrogen)[25], and for that to Gα, mGFP was fused to the N terminus of bovine Gα1 (a kind
268 gift from T. Haga of Gakushuin University) [26] in the pEGFP-C1 vector (Clontech), after the
269 removal of the cDNA region encoding EGFP. The details of the constructed cDNAs are shown
270 in **Extended Data Fig. 1**. The L cells were transfected with these cDNAs using
271 LipofectAMINE LTX (Life Technologies), according to the manufacturer's recommendations.
272 Transfected cells were seeded in glass-base dishes (35 mmϕ with a glass window of 12 mmϕ,
273 0.12~0.17-mm-thick glass; Iwaki), and cultured in Ham's F12 medium (Sigma-Aldrich),
274 supplemented with 10 % (v/v) FBS (Sigma-Aldrich), 100 units/ml penicillin (Wako), and 0.1
275 mg/ml streptomycin (Wako), for 24~48 h before microscope observations. The F12 medium
276 was employed because it has a lower fluorescence background as compared with DMEM,
277 which was used for routine culturing.

278 The agonist, isoproterenol (Sigma-Aldric), and the inverse agonists, ICI-118,551
279 (Tocris) and timolol (Wako), were dissolved in Hank's balanced salt solution (Nissui)
280 buffered with 2 mM piperazine-N,N'-bis(ethanesulfonic acid) (PIPES, Dojindo) at pH 7.4

281 (P-HBSS), at concentrations of 20, 200, and 200 μM, respectively. For the additions to the
282 cells, 1 ml solutions of these reagents were added to the cells in 1 ml of the Ham's F12
283 medium described above, providing the final concentrations of 10 μM isoproterenol, 100 μM
284 ICI-118,551, and 100 μM timolol.
285
286 **Labelling of β2AR with the fluorescent dye ATTO594**
287 ATTO594-Coenzyme A was custom-synthesised by Shinsei Kagaku, by conjugating
288 ATTO594-maleimide (ATTO-TECH) to Coenzyme A-SH (New England Biolabs), followed by
289 HPLC purification. The chemical structure of ATTO594-Coenzyme A was confirmed by liquid
290 chromatography-mass spectrometry (LC-MS; LCMS-2010A EV, Shimadzu). The ACP-tagged
291 β2AR expressed in the PM of the L cells was labelled with ATTO594, by incubating the cells
292 with 2 μM ATTO594-Coenzyme A and 1 μM phosphopantetheine transferase (New England
293 Biolabs) in Ham's F12 medium without FBS at ~25°C for 20 min. These conditions have
294 been known to achieve ~95% labelling of ACP[24]. The cells were washed with P-HBSS three
295 times, and then subjected to microscope observations. The cells exhibiting the presence of
296 ~3 ATTO594-ACP-B2AR spots/μm^2 in the PM were used for single-molecule imaging
297 experiments.
298
299 **Single fluorescent-molecule video imaging of live cells**
300 The fluorescently-labelled ACP-β2AR expressed in the bottom PM was observed at the level
301 of single molecules at 37°C, using home-built objective-lens-type total internal reflection
302 fluorescence microscopes based on Olympus IX-70, Olympus IX-81, or Nikon TE-2000
303 inverted microscopes[4,7,27,28], with a 100x objective lens, as optimised for the present
304 research. Fluorescence images were projected onto a two-stage microchannel plate
305 intensifier (C8600-03, Hamamatsu Photonics), coupled to an electron bombardment CCD
306 camera (C7190-23; Hamamatsu Photonics) or an sCMOS camera (ORCA-Flash 4.0;
307 Hamamatsu Photonics) operated at 30 Hz. For observations at a frame rate of 250 Hz, a
308 CMOS camera (FASTCAM 1024PCI-II, Photron) was employed[29]. Fluorescent spots were

309 identified by using an in-house computer program, as described previously[4]. The positions
310 (x and y coordinates) of all of the observed single fluorescent-molecules were determined
311 by a computer program that employed the method developed previously[30,31]. For the
312 simultaneous dual-color single-molecule imaging, the images were spectrally split into two
313 emission arms, each containing the same image intensifier and camera.
314 To maintain the cells at 37°C during the microscope observations, the entire
315 microscope, except for the two detection arms and the excitation arm, was placed in a
316 home-built microscope environment chamber made with thermo-insulating transparent
317 vinyl sheets, and three heating circulators (SKH0-112-OT, Kokensya) were appropriately
318 placed in the chamber to supply warmed air with slow circulation[28,32,33]. For further
319 stabilisation, a plate heater (INUG2, Tokai Hit) was mounted on the microscope stage. The
320 temperature of the surrounding air just above the stage was continually monitored during
321 the observations with a digital thermometer (DT-312, Intermedical).
322
323 **Detection of colocalisation-codiffusion, and evaluations of β2AR dimer lifetimes**
324 **and two-dimensional dissociation constants of β2AR dimers**
325 The number densities of β2AR molecules existing as (true) dimers and the number density
326 of the expressed β2AR molecules were determined by single-molecule imaging of
327 ATTO594-ACP-β2AR[4]. Colocalisations of two fluorescent spots (molecules) of the same color
328 (the same ATTO594 probe) or those of two different colors (YFP for BiFC and ATTO594)
329 were detected when the two fluorescent molecules became localised within 220 nm of each
330 other[4,28]. The number densities of incidental colocalisations at given molecular densities
331 were subtracted[4]. The two-dimensional dissociation constant (2D-K_D) of β2AR in the PM was
332 determined by using the method previously developed by us[4].
333 To directly detect the actual binding of two β2AR molecules, forming homo-dimers, we
334 employed the bimolecular fluorescence complementation (BiFC) method[4,34]. The details of
335 the BiFC method are described in the next subsection.

336 To determine the lifetime of β2AR dimers using single color observations (with
337 ATTO594-ACP-β2AR), the duration of each colocalisation-codiffusion event was
338 measured[4,12], and after the durations of many events were determined, histograms showing
339 the distribution of colocalisation durations were obtained. All of the histograms obtained
340 from the image sequences obtained at a time resolution of 33 ms could be fitted by single
341 exponential functions, which provided decay time constants (lifetime; τ_{observed}). τ_{observed} was
342 then corrected for the photobleaching lifetime of the fluorescent probe ATTO594 (τ_{bleach} =
343 7.21 ± 0.81 s for 30 Hz [n = 300] and 0.812 ± 0.041 s for 250 Hz [n = 539]), to obtain the
344 duration of apparent colocalisation ($\tau_{apparent\ colocalisation}$), using the equation [$\tau_{observed}^{-1}$ -
345 $2\tau_{bleach}^{-1}]^{-1}$ [4,7,12]. The effective dimer lifetime or the effective binding lifetime of proteins, τ,
346 was evaluated by subtracting the duration of incidental colocalisation (without specific
347 molecular interactions; $\tau_{incidental}$) from $\tau_{apparent\ colocalisation}$. For details, see our previous
348 publications[4,7]. $\tau_{incidental}$ was evaluated by using a monomer reference molecule, ACP linked
349 to the transmembrane domain of the low-density lipoprotein receptor, called ACP-TM[7], and
350 was found to be 19 ± 0.46 ms (exponential lifetime; n = 241 examined dimers; 39 examined
351 movies; No. of Freedoms = 97).
352
353 **Observations of the recruitment of Gαs and Gβγ to βAR monomers and dimers**
354 The recruitment of Gαs and Gβγ to βAR monomers and dimers was detected by observing
355 the colocalisation-codiffusion of mGFP-conjugated Gαs and Gβγ with ATTO594-labelled
356 β2AR monomers and dimers, at the level of single molecules. The colocalisation events
357 lasting for longer than 66 ms (2 video frames) were analysed. The frequency of incidental
358 colocalisation was estimated by superimposing an image sequence with one color on
359 another image sequence with a different color that was artificially shifted by ~500 nm
360 (horizontally), and was subtracted. The recruitment frequencies of Gαs and Gβγ to βAR
361 monomers and dimers (per sec per μm^2) were normalised by the number densities of Gαs
362 (or Gβγ) and β2AR protomers in the PM.
363

364 **The BiFC method for examining the formation of β2AR dimers (the interaction of**
365 **two β2AR molecules at the molecular level)**
366 The YFP-based BiFC(N) and BiFC(C) moieties employed previously[4,35] were respectively
367 fused to the C terminus of ACP-β2AR (**Extended Data Fig. 1**) in the pEGFP-N1 vector
368 (Invitrogen; the cDNA region encoding EGFP was removed). These proteins were
369 co-expressed in L cells, by transfection with LipofectAMINE LTX (Life Technologies)
370 according to the manufacturer's recommendations, and then ATTO594 was conjugated to
371 the ACP moieties of ACP-β2AR-BiFC(N) and BiFC(C). As the monomer reference molecule for
372 the BiFC data, ACP-TM was employed and the YFP-based BiFC(N) and BiFC(C) moieties were
373 fused to the C terminus of ACP-TM, as previously described[4]. Using dual-color
374 single-molecule imaging (ATTO594 and mGFP), the number densities of the expressed
375 molecules (the sum of the number densities of ACP-conjugated molecules) and those of the
376 fluorescence spots of reconstituted BiFC molecules (spots/μm^2) were determined.
377
378 **Evaluation of the changes of the cytosolic cAMP levels**
379 The amounts of cAMP in the cytosol were measured by using the time-resolved fluorescence
380 resonance energy transfer (TR-FRET) kit from Perkin Elmer (EnVision Xcite), according to
381 the manufacturer's recommendations. Since the L cells used for single-molecule
382 experiments expressed very low levels of β2AR, and thus the basal level of cAMP in the
383 resting state was below the detection limit, we first established a stable L-cell line
384 expressing β2AR at high levels[36], and used these cells to evaluate the changes of the cAMP
385 levels in the cytosol before and after the additions of the agonist and inverse agonists. The
386 drug treatments were performed as described at the end of the subsection, "Cell culture,
387 cDNA construction and expression in L cells, and treatment of cells with agonists and inverse
388 agonists".
389
390 **Generation of artificial β2AR dimers and observations of Ca^{2+} mobilisation**
391 To artificially generate stable homo-dimers of β2AR, we employed a chemical dimerising

392 system based on the FK506-binding protein (FKBP)-ligand interface[37]. First, the cDNA
393 encoding Halo7-β2AR-FKBP_F36V (β2AR-FKBP) was cloned into the expression plasmid
394 vector pEGFP-N1 (Clontech) after the removal of the cDNA region encoding EGFP, and then
395 the cDNA encoding FKBP_F36V was replaced by the cDNA encoding FKBP (obtained from
396 the YFP-FKBP cDNA, the Addgene plasmid 20175 donated by T. Meyer[38]). Halo7-β2AR-FKBP
397 expressed in L cells was fluorescently labelled by incubating the cells for 24 - 48 h with 5 nM
398 Halo-tag conjugated with SaraFluor 650T (Goryo-Kayaku;
399 SaraFluor650T-Halo7-β2AR-FKBP). The crosslinker for FKBP, AP20187 (Takara), was added
400 at a final concentration of 5 nM during the image acquisition, and dimer formation was
401 detected at the level of single molecules.
402 For Ca^{2+} mobilisation assays, a freshly-prepared 1 mg/ml DMSO solution of Fluo4-AM
403 (Dojindo) was added to HBSS buffered with 10 mM
404 (4-(2-hydroxyethyl)-1-piperazineethanesulfonic acid) at pH 7.4 (H-HBSS), containing 1.25
405 mM Probenecid (Dojindo) and 0.04 % (w/v) Pluronic F127 (Dojindo) (loading buffer), to
406 obtain a final Fluo4-AM concentration of 5 μg/ml (4.6 μM), basically following the
407 manufacturer's recommendations. The L cells prepared as above for detecting dimers of
408 SaraFluor650T-Halo7-β2AR-FKBP at the single-molecule level were incubated with the
409 loading buffer at 37°C for 1 h and washed with H-HBSS three times, and then 500 μl
410 H-HBSS was added for epi-fluorescence microscopic observations. Fluo4 fluorescence was
411 recorded at 2 Hz. The stable dimers of SaraFluor650T-Halo7-β2AR-FKBP were induced by
412 the addition of 5 nM AP20187, as described above. To determine the saturation levels of the
413 fluorescence signal intensity of Fluo4 at higher concentrations of Ca^{2+}, 1 μM (final
414 concentration) ionomycin (Wako) was added to the cells to equalise the intracellular Ca^{2+}
415 concentrations with that outside the cells (1.3 mM).
416
417 **Software and statistical analysis**
418 Superimpositions of image sequences obtained from dual-color single fluorescent molecule
419 observations and single fluorescent spot tracking were performed using C++-based

computer programs produced in-house, as described previously[28,30]. Statistical analysis was performed by the two-sided Welch's t test (except for the data shown in **Extended Data Fig. 5c**, where the one-sided t test was used) or the Brunner-Munzel statistical test, by using the R Studio Software (R Foundation for Statistical Computing, https://www.R-project.org/). *P* values less than 0.05 were considered to be statistically significant. Linear and non-linear curve fittings were performed by using OriginPro 9.1 for Windows, with appropriate scripts.

Data and code availability

All data generated or analysed for this study are available within the paper and its associated Extended Data Figures and Tables. All other data presented and software codes are available upon request from the corresponding author. A **Reporting Summary** for this paper is available.

435 **References**

436 1 Seifert, R. & Wenzel-Seifert, K. Constitutive activity of G-protein-coupled receptors: cause of
437 disease and common property of wild-type receptors. *Naunyn-Schmiedeberg's Arch.*
438 *Pharmacol.* **366**, 381-416 (2002).

439 2 Nakashima, A. *et al.* Agonist-independent GPCR activity regulates anterior-posterior
440 targeting of olfactory sensory neurons. *Cell* **154**, 1314-1325 (2013).

441 3 Wacker, D., Stevens, R.C. & Roth, B.L. How Ligands Illuminate GPCR Molecular
442 Pharmacology. *Cell* **170**, 414-427 (2017).

443 4 Kasai, R.S. *et al.* Full characterization of GPCR monomer-dimer dynamic equilibrium by single
444 molecule imaging. *J. Cell Biol.* **192**, 463-480 (2011).

445 5 Calebiro, D. *et al.* Single-molecule analysis of fluorescently labeled G-protein-coupled
446 receptors reveals complexes with distinct dynamics and organization. *Proc. Natl. Acad. Sci.*
447 *USA* **110**, 743-748 (2013).

448 6 Hern, J.A. *et al.* Formation and dissociation of M1 muscarinic receptor dimers seen by total
449 internal reflection fluorescence imaging of single molecules. *Proc. Natl. Acad. Sci. USA* **107**,
450 2693-2698 (2010).

451 7 Kasai, R.S., Ito, S.V., Awane, R.M., Fujiwara, T.K. & Kusumi, A. The Class-A GPCR Dopamine
452 D2 Receptor Forms Transient Dimers Stabilized by Agonists: Detection by Single-Molecule
453 Tracking. *Cell Biochem. Biophys.* **76**, 29-37 (2018).

454 8 Tabor, A. *et al.* Visualization and ligand-induced modulation of dopamine receptor
455 dimerization at the single molecule level. *Sci. Rep.* **6**, 33233 (2016).

456 9 James, J.R., Oliveira, M.I., Carmo, A.M., Iaboni, A. & Davis, S.J. A rigorous experimental
457 framework for detecting protein oligomerization using bioluminescence resonance energy
458 transfer. *Nat. Methods* **3**, 1001-1006 (2006).

459 10 Mercier, J.F., Salahpour, A., Angers, S., Breit, A. & Bouvier, M. Quantitative assessment of
460 beta 1- and beta 2-adrenergic receptor homo- and heterodimerization by bioluminescence
461 resonance energy transfer. *J. Biol. Chem.* **277**, 44925-44931 (2002).

462 11 Tennenberg, S.D., Zemlan, F.P. & Solomkin, J.S. Characterization of

463 N-formyl-methionyl-leucyl-phenylalanine receptors on human neutrophils. Effects of isolation
464 and temperature on receptor expression and functional activity. *J. Immunol.* **141**,
465 3937-3944 (1988).
466 12 Suzuki, K.G. *et al.* Transient GPI-anchored protein homodimers are units for raft organization
467 and function. *Nat. Chem. Biol.* **8**, 774-783 (2012).
468 13 Meyer, B.H. *et al.* FRET imaging reveals that functional neurokinin-1 receptors are
469 monomeric and reside in membrane microdomains of live cells. *Proc. Natl. Acad. Sci. USA*
470 **103**, 2138-2143 (2006).
471 14 Katritch, V., Cherezov, V. & Stevens, R.C. Structure-function of the G protein-coupled
472 receptor superfamily. *Annu. Rev. Pharmacool. Toxicol.* **53**, 531-556 (2013).
473 15 Ballesteros, J.A. *et al.* Activation of the beta 2-adrenergic receptor involves disruption of an
474 ionic lock between the cytoplasmic ends of transmembrane segments 3 and 6. *J. Biol. Chem.*
475 **276**, 29171-29177 (2001).
476 16 O'Dowd, B.F. *et al.* Site-directed mutagenesis of the cytoplasmic domains of the human beta
477 2-adrenergic receptor. Localization of regions involved in G protein-receptor coupling. *J. Biol.*
478 *Chem.* **263**, 15985-15992 (1988).
479 17 Sungkaworn, T. *et al.* Single-molecule imaging reveals receptor-G protein interactions at cell
480 surface hot spots. *Nature* **550**, 543-547 (2017).
481 18 Schmidt, M. *et al.* A new phospholipase-C-calcium signalling pathway mediated by cyclic AMP
482 and a Rap GTPase. *Nat. Cell Biol.* **3**, 1020-1024 (2001).
483 19 Kalay, Z., Fujiwara, T.K. & Kusumi, A. Confining domains lead to reaction bursts: reaction
484 kinetics in the plasma membrane. *PloS one* **7**, e32948 (2012).
485 20 Kusumi, A. *et al.* Dynamic organizing principles of the plasma membrane that regulate signal
486 transduction: commemorating the fortieth anniversary of Singer and Nicolson's fluid-mosaic
487 model. *Annu. Rev. Cell Dev. Biol.* **28**, 215-250 (2012).
488 21 Kusumi, A. *et al.* Paradigm shift of the plasma membrane concept from the two-dimensional
489 continuum fluid to the partitioned fluid: high-speed single-molecule tracking of membrane
490 molecules. *Annu. Rev. Biophys. Biomol. Struct.* **34**, 351-378 (2005).

491 22 Davenport, A.P. *et al.* International Union of Basic and Clinical Pharmacology. LXXXVIII. G
492 protein-coupled receptor list: recommendations for new pairings with cognate ligands.
493 *Pharmacol. Rev.* **65**, 967-986 (2013).
494 23 Dixon, R.A. *et al.* Ligand binding to the beta-adrenergic receptor involves its rhodopsin-like
495 core. *Nature* **326**, 73-77 (1987).
496 24 George, N., Pick, H., Vogel, H., Johnsson, N. & Johnsson, K. Specific labeling of cell surface
497 proteins with chemically diverse compounds. *J. Am. Chem. Soc.* **126**, 8896-8897 (2004).
498 25 Yu, J.Z. & Rasenick, M.M. Real-time visualization of a fluorescent G(alpha)(s): dissociation of
499 the activated G protein from plasma membrane. *Mol. Pharmacol.* **61**, 352-359 (2002).
500 26 Janetopoulos, C., Jin, T. & Devreotes, P. Receptor-mediated activation of heterotrimeric
501 G-proteins in living cells. *Science* **291**, 2408-2411 (2001).
502 27 Iino, R., Koyama, I. & Kusumi, A. Single molecule imaging of green fluorescent proteins in
503 living cells: E-cadherin forms oligomers on the free cell surface. *Biophys. J.* **80**, 2667-2677
504 (2001).
505 28 Koyama-Honda, I. *et al.* Fluorescence imaging for monitoring the colocalization of two single
506 molecules in living cells. *Biophys. J.* **88**, 2126-2136 (2005).
507 29 Hiramoto-Yamaki, N. *et al.* Ultrafast diffusion of a fluorescent cholesterol analog in
508 compartmentalized plasma membranes. *Traffic* **15**, 583-612 (2014).
509 30 Fujiwara, T., Ritchie, K., Murakoshi, H., Jacobson, K. & Kusumi, A. Phospholipids undergo
510 hop diffusion in compartmentalized cell membrane. *J. Cell Biol.* **157**, 1071-1081 (2002).
511 31 Gelles, J., Schnapp, B.J. & Sheetz, M.P. Tracking kinesin-driven movements with
512 nanometre-scale precision. *Nature* **331**, 450-453 (1988).
513 32 Murakoshi, H. *et al.* Single-molecule imaging analysis of Ras activation in living cells. *Proc.*
514 *Natl. Acad. Sci. USA* **101**, 7317-7322 (2004).
515 33 Tsunoyama, T.A. *et al.* Super-long single-molecule tracking reveals
516 dynamic-anchorage-induced integrin function. *Nat. Chem. Biol.* **14**, 497-506 (2018).
517 34 Hu, C.D., Chinenov, Y. & Kerppola, T.K. Visualization of interactions among bZIP and Rel
518 family proteins in living cells using bimolecular fluorescence complementation. *Mol. Cell* **9**,

519 789-798 (2002).
520 35 Briddon, S.J. & Hill, S.J. Pharmacology under the microscope: the use of fluorescence
521 correlation spectroscopy to determine the properties of ligand-receptor complexes. *Trends*
522 *Pharmacol. Sci.* **28**, 637-645 (2007).
523 36 Yusa, K., Zhou, L., Li, M.A., Bradley, A. & Craig, N.L. A hyperactive piggyBac transposase for
524 mammalian applications. *Proc. Natl. Acad. Sci. USA* **108**, 1531-1536 (2011).
525 37 Clackson, T. *et al.* Redesigning an FKBP-ligand interface to generate chemical dimerizers with
526 novel specificity. *Proc. Natl. Acad. Sci. USA* **95**, 10437-10442 (1998).
527 38 Inoue, T., Heo, W.D., Grimley, J.S., Wandless, T.J. & Meyer, T. An inducible translocation
528 strategy to rapidly activate and inhibit small GTPase signaling pathways. *Nat. Methods* **2**,
529 415-418 (2005).
530
531

Fig. 1

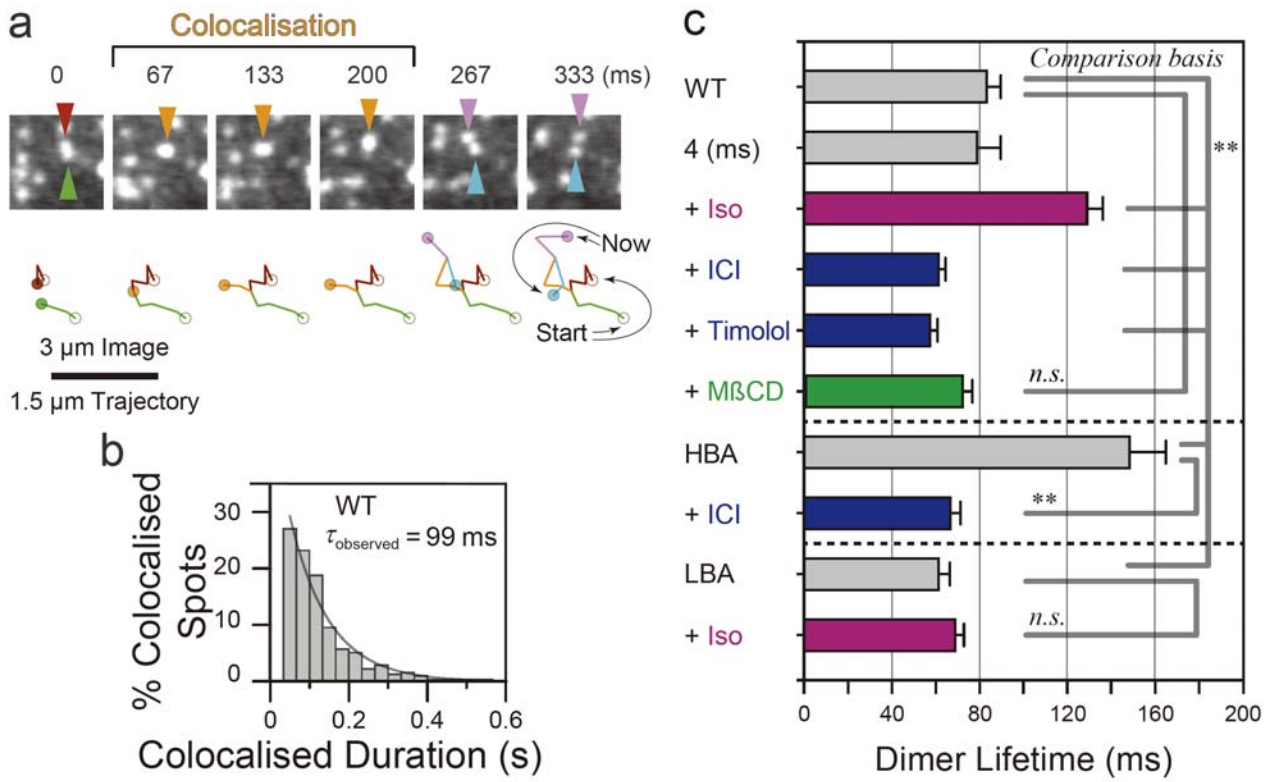

Fig. 1. β2AR dynamically interconverts between monomers and transient homodimers. Mean, SEM, the number of experiments, and other statistical parameters are summarised in **Extended Data Table 1**.

(a) A typical snapshot sequence (among 13 movies) showing transient homo-dimerisation of β2AR molecules. Two molecules became colocalised at frame 2 (67 ms), diffused together for 134 ms (colocalisation), and then separated.

(b) Histogram showing the distribution of the durations of the WT-β2AR colocalisation events (homo-dimers). Note that the $\tau_{observed}$ is the value before corrections for photobleaching and incidental colocalisations.

(c) Summary of the dimer lifetimes (after corrections) of WT and mutant β2AR obtained before and after the additions of various reagents. ** and *n.s.*: statistically significant and non-significant with *P* values smaller or greater than 0.05, respectively. This convention was used throughout this report.

Fig. 2

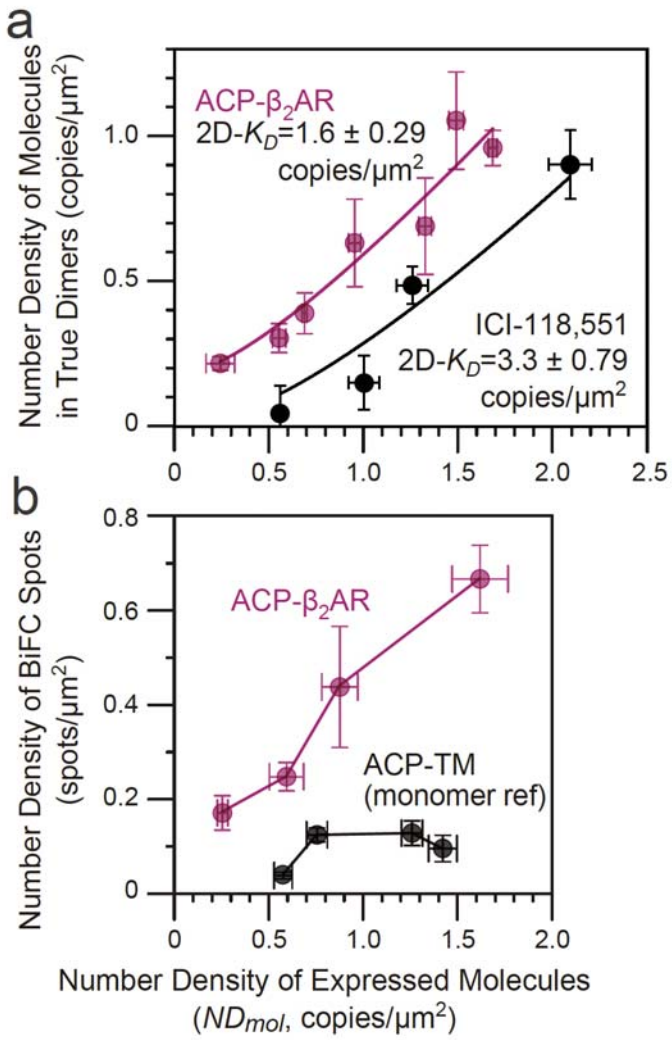

Fig. 2. Determining the 2D-*K*D of β2AR dimers with/without an inverse agonist and the BiFC detection of β2AR dimers. Mean, SEM, the number of experiments, and other statistical parameters are summarised in **Extended Data Table 2**.

The number density of β2AR molecules in true dimers (after subtraction of incidental overlap of fluorescent spots; ± inverse agonist; fitted with Eq. 5 in Ref4; red curve) **(a)** and the number densities of the BiFC spots for ACP-β2AR-YFP(N/C) and ACP-TM-YFP(N/C) (monomer reference molecule) **(b)**, plotted as a function of the number density of expressed molecules (*NDmol*). In **b**, the lines are provided to facilitate visualisation.

Fig. 3

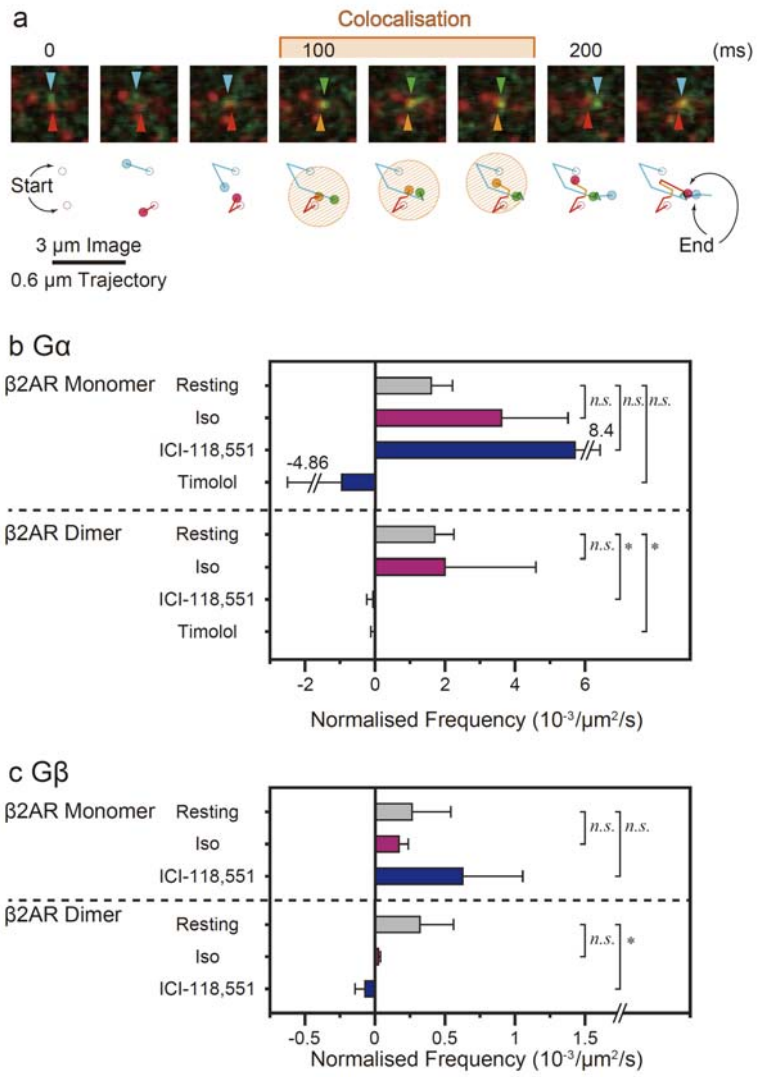

Fig. 3. Non-stimulated β2AR homo-dimers recruit trimeric G-proteins: a process suppressed by inverse agonists. Mean, SEM, the number of experiments, and other statistical parameters are summarised in **Extended Data Table 3**.

(a) A typical snapshot image sequence (among 40 movies) showing that a trimeric G-protein Gαs subunit transiently binds to a β2AR monomer.

(b, c) The inverse agonists, ICI-118,551 and Timolol, inhibitors of β2AR basal constitutive activities, blocked the recruitment of trimeric G-proteins to β2AR homo-dimers, but not that to monomers. Gαs **(b)** and Gβγ **(c)** colocalisation frequencies with β2AR monomers and homo-dimers. The normalised frequencies of colocalisations = the number of colocalisation events per sec per μm^2 normalised by the number densities of Gαs (or Gβγ) and β2AR protomers.